PROTOTYPE DESIGN AND EXPERIMENTAL VERIFICATION OF AN ELECTROMAGNETIC ACTUATOR FOR PARAMETRIC STIFFNESS EXCITATION

Erich Schmidt, *Member*, *IEEE*[1], Horst Ecker[2]

[1]Institute of Electrical Drives and Machines, Vienna University of Technology, Vienna, Austria
erich.schmidt@tuwien.ac.at

[2]Institute of Mechanics and Mechatronics, Vienna University of Technology, Vienna, Austria
horst.ecker@tuwien.ac.at

Abstract – Initial design, realization and application of a novel electromagnetic actuator to create a time-harmonic variation of a mechanical stiffness will be discussed. It is known from theoretical studies, that such a time-periodic parameter variation at a non-resonant parametric resonance frequency can improve the damping behaviour of a mechanical system. Thus, a device consisting of a current driven coil positioned between two permanent magnets has been designed and tested. Finite element analyses have been carried out to obtain the mechanical stiffness provided as a function of the coil current excitation. With this novel electromagnetic actuator it is possible to demonstrate the improved damping behaviour of a mechanical two-mass system, when the actuator is operating at or near a certain parametric combination resonance frequency.

Keywords – Electromagnetic actuator, electromagnetic forces, parametric excitation, vibration damping

1. INTRODUCTION

In most cases, physical systems in the fields of electrical and mechanical engineering can either be described by linear differential equations with constant (i.e. time-invariant) parameters (LTI-systems) or by linear differential equations with time-varying coefficients (LTV-systems).

Basically, the generic equation of motion of a certain class of mechanical systems with lumped parameters and parametric stiffness excitation can be written as

$$\mathbf{M}\,\ddot{\mathbf{x}}(t) + \mathbf{C}\,\dot{\mathbf{x}}(t) + \mathbf{K}\,\mathbf{x}(t) + \mathbf{K}_{PSE}(t)\,\mathbf{x}(t) = \mathbf{0} \ . \quad (1)$$

Therein, $\mathbf{M}$, $\mathbf{C}$, $\mathbf{K}$ denote mass, damping and stiffness matrix of the mechanical system [1]. In the work presented here, only single-frequency excitation is considered. Thus, the parametric stiffness excitation represented by $\mathbf{K}_{PSE}(t)$ shows a time-harmonic variation as

$$K_{PSE,ij}(t) \sim \cos\big(\omega_{PSE}\,t + \varphi_{ij}\big) \ . \quad (2)$$

LTV-systems as in (1) with more than two state variables lead to larger sets of system equations and consequently to a rather complex behaviour with respect to parametric resonances [2]. Due to the increased number of eigenvalues of such systems, various frequencies of parametric resonances are observed. A system with parametric excitation may exhibit *principle parametric resonances* at frequencies

$$\omega^{pr}_{j,k} = \frac{2\Omega_j}{k} \ , \quad j = 1, \ldots, n \ , \quad (3)$$

and *combination parametric resonances* at frequencies

$$\omega^{cr}_{i\pm j,k} = \frac{\big|\Omega_i \pm \Omega_j\big|}{k} \ , \quad i \neq j \ , \ i, j = 1, \ldots, n \ . \quad (4)$$

Therein, Ω_i and Ω_j denote the i-th (j-th) natural frequencies of the system of order n, obtained from the undamped eigenvalue problem

$$\mathbf{M}\,\ddot{\mathbf{x}}(t) + \mathbf{K}\,\mathbf{x}(t) = \mathbf{0} \ . \quad (5)$$

The denominator $k \in \mathcal{N}$ represents the order of the parametric resonance. Most of the time, only first order resonances $k = 1$ of the two lowest frequencies Ω_1 and Ω_2 are significant.

Parametric resonances may be resonant or non-resonant. In the resonant case, a mechanical system would experience large vibration amplitudes which may be strong enough to cause serious damage on a machine. Thus, parametric resonances are commonly considered as unwanted or even dangerous under certain circumstances.

Non-resonant parametric resonances may occur at certain frequencies $\omega^{cr}_{i\pm j,k}$ and simply do not cause any vibration amplitude amplification. Based on early works of A. Tondl, it is known that non-resonant parametric resonances are not only just non-resonant but an even faster decay of vibration amplitudes may occur at these frequencies [3]. Thus, it is possible to take advantage of this phenomenon and to stabilize an unstable system by introducing a parametric excitation at a non-resonant parametric resonance frequency [4], [5].

Nowadays, analytical and numerical methods have been applied extensively and results show that parametric excitation can significantly enhance the damping properties of a system [1], [6]. To prove the above mentioned effect and the theoretical results in an experiment it is necessary to vary a certain physical parameter of the investigated system periodically. Among the parameters available with a mechanical systems it is very effective to choose a stiffness element in the system for this purpose.

2. DESIGN OF THE ELECTROMAGNETIC ACTUATOR

There are various possibilities to create a mechanical element with time-dependent stiffness. It has been shown that a pure mechanical realization of an applicable parametric stiffness excitation is possible, but such a device has to be designed quite carefully to avoid unwanted friction effects and other disturbances [1], [7]. Therefore, a different approach based on the repellent forces that can be created by two magnetic fields is concerned.

If the same poles of two magnetic fields approach each other, repellent forces are generated, which increase with decreasing distance. This reaction is similar to that of a mechanical spring which is compressed. If one (or both) of the magnetic fields is modulated, then a time-periodic stiffness can be created. This is the basic idea of the electromagnetic actuator which was designed for the purpose of creating a time-varying stiffness element in a mechanical arrangement.

Fig. 1 depicts a schematic of the actual design of this actuator. Inside the cylindrical ferromagnetic housing (4) at both ends two ring-shaped NdFeB permanent magnets (2) with axial magnetization in the same direction are installed. In the open space inside the housing and between the two permanent magnets, a current driven coil (1) mounted on a high-strength carbon-fibre rod (3) can travel freely in both axial directions. The non-magnetic rod extends through the holes of both magnets and is supported (5) outside of the housing.

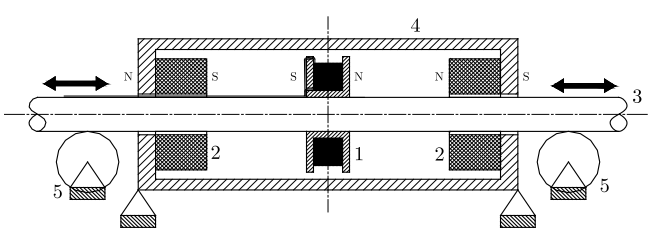

Fig. 1: Schematic arrangement of the electromagnetic actuator with a moving current driven coil (1) between two permanent magnets (2), a carbon fibre rod (3), a ferromagnetic housing (4) and the linear support (5)

The desired time-varying stiffness is obtained from a current excitation with a time-constant DC part and a time-harmonic AC part according to the parametric resonance frequency.

2.1. Finite Element Analysis

Due to the cylindrical arrangement, a 2D model with a rotational symmetry is sufficient to give accurate results. As proposed in [8]–[10], the constitutive relation can be written as

$$\vec{H} = \nu(\vec{B})\,\vec{B} \ , \tag{6}$$

and the magnetic vector potential $\vec{A}$ is introduced as

$$\vec{B} = \operatorname{curl}\vec{A} \ . \tag{7}$$

The NdFeB permanent magnets are designed for very high energy densities and show a remanent magnetic flux density of $B_r = 1.35\,\mathrm{T}$ as well as a coercive magnetic field strength of $H_c = 955\,\mathrm{kA/m}$. The coil current excitation is represented with an impressed current density in circumferential direction according to the total magnetomotive force of the coil.

Fig. 2 depicts the distribution of the magnetic flux density and the magnetic flux tubes of the two permanent magnets without a coil current excitation. Based on the strong magnetization of both magnets, the ferromagnetic housing will guide most of the magnetic flux generated from the permanent magnets. This will cause only a slight change of the magnetic field linkage of the coil in case of a current excitation.

2.2. Force Calculation

The Maxwell stress tensor

$$\underset{\sim}{p} = \frac{1}{2\mu_0}\big(\vec{B}\cdot\vec{B}\big)\,\underset{\sim}{\delta} - \frac{1}{\mu_0}\big(\vec{B}\otimes\vec{B}\big) \ . \tag{8}$$

will be used to obtain both the acting local volume and surface force densities [10], [11]. Taking into account for $\operatorname{curl}\vec{H} = \vec{J}$ and the continuity of the magnetic field vectors, the volume force density acting within the current carrying regions and the surface force density acting at the non-magnetic coil surroundings can be calculated from

$$\vec{f}^{\,v} = -\nabla\cdot\underset{\sim}{p} = \vec{J}\times\vec{B} \ , \tag{9}$$

$$\vec{f}^{\,s} = -\vec{n}\cdot\underset{\sim}{p} = \frac{1}{2\mu_0}\Big(2\big(\vec{n}\cdot\vec{B}\big)\vec{B} - \big(\vec{B}\cdot\vec{B}\big)\vec{n}\Big) \ , \tag{10}$$

where $\vec{n}$ denotes the normal vector oriented from the coil regions to the surrounding air regions.

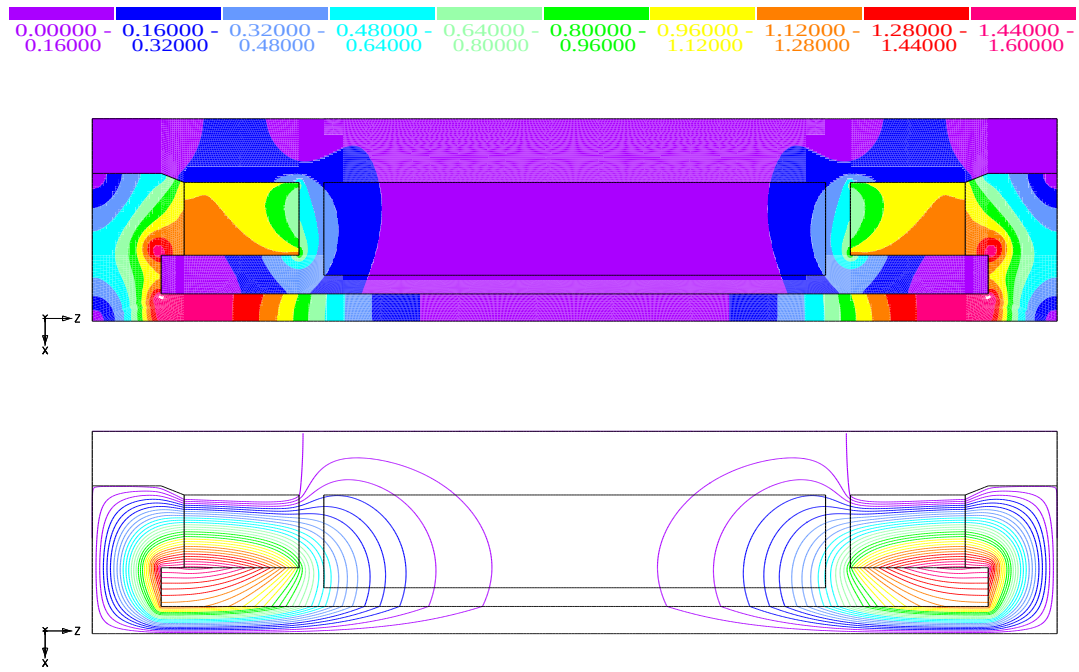

Fig. 2: Magnetic flux density (upper part) and magnetic flux tubes (lower part) of the two permanent magnets without coil current excitation

2.3. Analysis Results

Due to the above mentioned fact about the dominant magnetic field of the permanent magnets, the force acting on the coil strongly depends on the current excitation with a linear characteristic. This is clearly depicted in Fig. 3 and Fig. 4. In addition to the finite element results, the results from measurements of the mechanical stiffness are shown. Obviously, there is a very good agreement of both stiffness results.

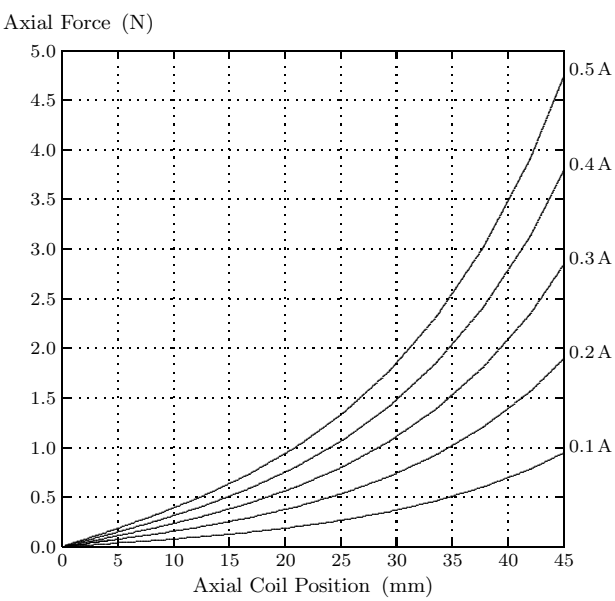

Fig. 3: Axial electromagnetic force as a function of deflection and coil current, finite element results

The nearly perfect linearity with regard to the coil current yields the analytical approximation of the mechanical stiffness achieved by the electromagnetic actuator as a function of the deflection as

$$k(i,x) = c_i\, i(t) \left(1 + c_x\, x^2(t)\right) \ , \tag{11}$$

where the constants are evaluated as $c_x = 872\,\mathrm{m}^{-2}$ and $c_i = 220/3\,\mathrm{N/(Am)}$.

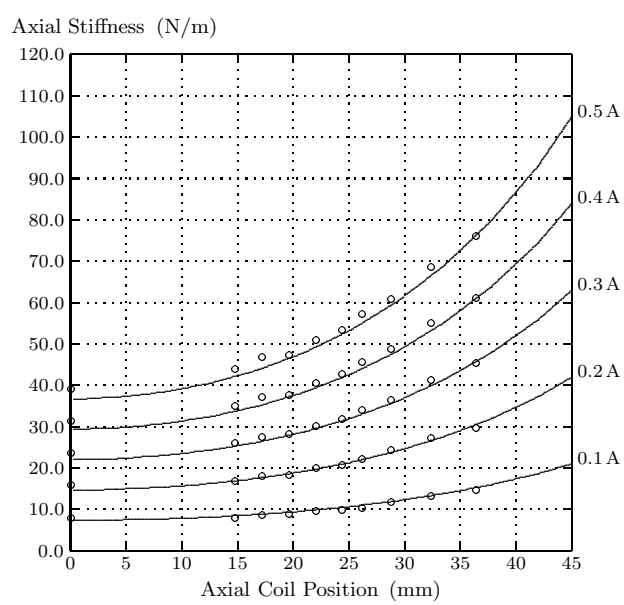

Fig. 4: Axial stiffness as a function of deflection and coil current, finite element results (solid lines) and measurement results (circles)

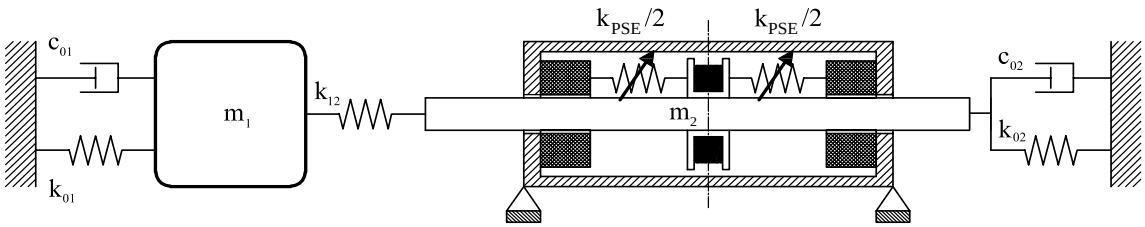

Fig. 5: Schematic of the experimental setup of the two-mass system with an electromagnetic actuator providing an additional time-varying stiffness $k_{PSE}(t) = k_0 + \hat{k}_{PSE}\ \cos(\omega_{PSE}\, t + \varphi_0)$

3. EXPERIMENTAL SETUP AND MEASUREMENT RESULTS

The electromagnetic actuator is part of a vibrational system with two masses m_1 and m_2, as shown in the sketch of Fig. 5. Mass m_1 is floating on an air-track to achieve minimal friction forces. Each mass is connected to the inertia reference frame by conventional coil springs k_{01} and k_{02}. A third coil spring k_{12} connects both masses. The damper element c_{02} represents an adjustable eddy current damper, whereas parameter c_{01} symbolizes the rather small damping originating from the air-track. Finally, the moving coil is driven by the time-dependent current

$$i(t) = i_0 + i_\sim\ \cos\omega_{PSE} t\ . \tag{12}$$

Table I lists the actual parameters of this test stand.

TABLE I
PARAMETER VALUES OF THE TEST STAND

Mass m_1	1.526	kg
Mass m_2	0.490	kg
Stiffness k_{01}	13.3	N/m
Stiffness k_{02}	20.0	N/m
Stiffness k_{12}	16.5	N/m
Damping c_{01}	0.017	Ns/m
Damping c_{02}	0.385	Ns/m
DC current i_0	0.3	A
AC current $i_\sim$	0.1	A
Frequency ω_{PSE}	5.28	rad/s

The electromagnetic actuator provides a constant stiffness k_0 which is related to the constant current i_0 by the relationship as shown with Fig. 4. The time-varying component of $i(t)$ creates a stiffness variation with the frequency of ω_{PSE} and a stiffness amplitude related to $i_\sim$. Since the actuator stiffness also depends on the coil position $x(t)$, the actual function of actuator stiffness versus time is not a single-frequency harmonic function as desired. Depending on the harmonic components of the coil deflection, various additional frequencies are generated. This is important to keep in mind, since the theoretical studies so far always assumed a single-frequency parametric excitation, which cannot be achieved with the actuator when operated the way as discussed here.

Numerous experiments have been carried out with the test stand, see [7], where a few typical results are shown here. In all experiments, both masses are deflected in the same direction and then released to oscillate freely until vibrations have vanished. In the case where the parametric stiffness excitation should be active, it is turned on when both masses are released.

Fig. 6 and Fig. 7 show time series of the deflections of mass 1 and mass 2 when parametric stiffness excitation was not active. Basically, both diagrams show free first-mode oscillations of the masses where the oscillations vanish after about 32 seconds. The final part of the signal obtained from mass 2 shows that disturbing friction effects created by the axial guidance of the actuator become significant at very small vibration amplitudes and determine more or less, when the vibration stops.

Fig. 8 and Fig. 9 show another time-series, obtained for identical test conditions as before, except that now the actuator is operated at the anti-resonance frequency (4) $\omega_{PSE} = \Omega_2 - \Omega_1$. By comparison with the previous results, a significant reduction of about 10 seconds for the decay time of the oscillations is achieved. This result demonstrates that the theoretically predicted effect of enhanced damping at a parametric anti-resonance can be proved experimentally. It is interesting to note that the oscillation amplitudes at mass 1 decay monotonically, whereas amplitudes at mass 2 become even larger for a short period of time and then decay very fast. Obviously, the parametric excitation transfers vibrational energy to mass 2 where it can be dissipated faster due to the eddy current damper attached to that mass.

4. CONCLUSION

A novel electromagnetic actuator to create a time-harmonic variation of a mechanical stiffness is presented. The obvious advantage of the electromagnetic actuator in comparison with pure mechanical realization is the fact that no moving mechanical parts are needed to generate the desired damping effect. The time-varying stiffness can easily be obtained from an according time-harmonic coil current excitation by an open-loop control. On the other hand, a major disadvantage is the

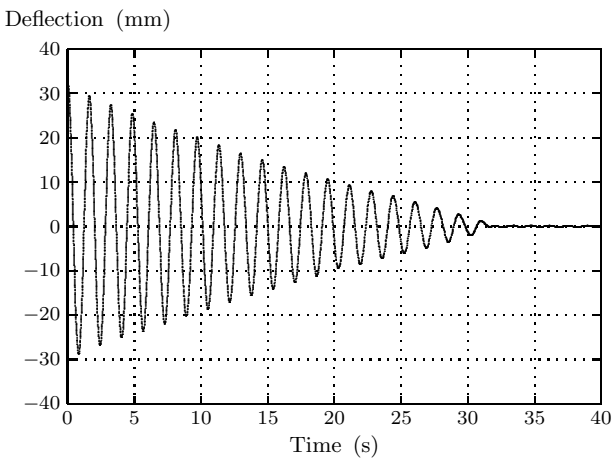

Fig. 6: Transient oscillation of mass 1 after an initial deflection with inactive parametric stiffness excitation

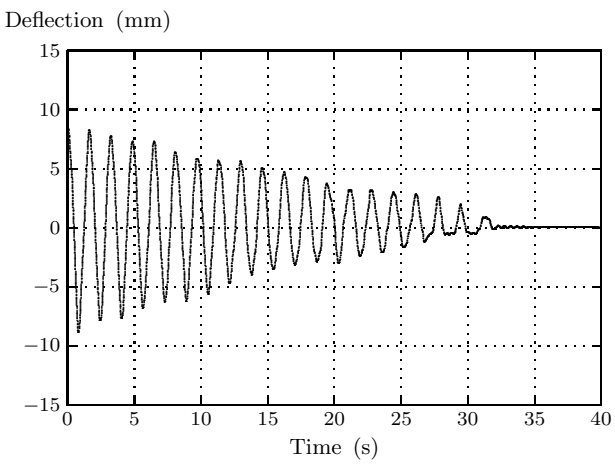

Fig. 7: Transient oscillation of mass 2 after an initial deflection with inactive parametric stiffness excitation

non-linearity of the achieved stiffness in relation to the deflection of the actuator coil.

As shown, the results of the finite element analysis, in particular in terms of the mechanical stiffness provided with the actuator, show a very good agreement with the results obtained from measurements. This way, the desired behaviour of the parametric stiffness excitation can be calculated in advance in a very accurate way.

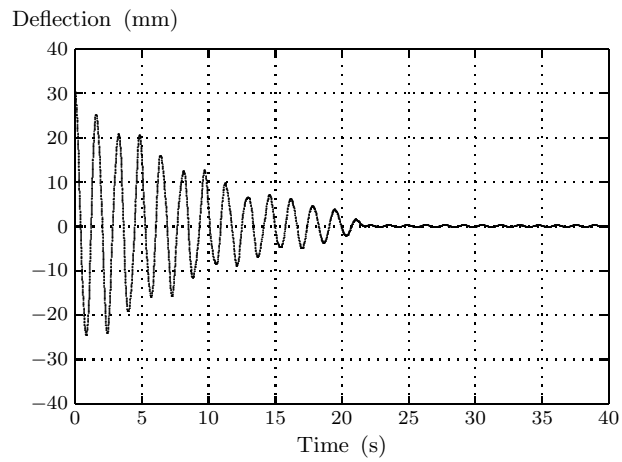

Fig. 8: Transient oscillation of mass 1 after an initial deflection with a parametric stiffness excitation at the anti-resonance frequency $\Omega_2 - \Omega_1$

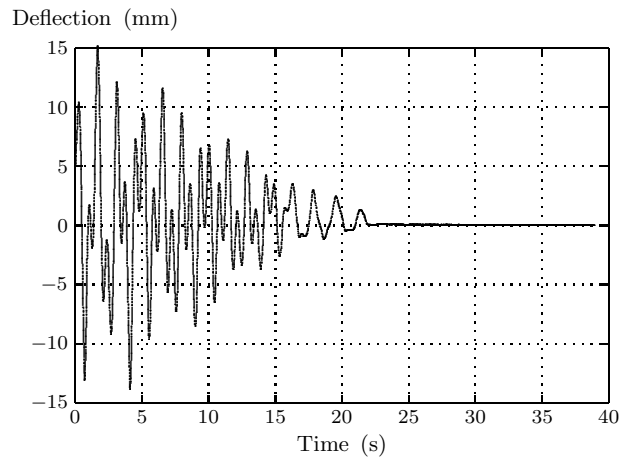

Fig. 9: Transient oscillation of mass 2 after an initial deflection with a parametric stiffness excitation at the anti-resonance frequency $\Omega_2 - \Omega_1$

REFERENCES

[1] Dohnal F., Paradeiser W., Ecker H.: "Experimental Study on Cancelling Self-Excited Vibrations by Parametric Excitation". *Proceedings of ASME 2006 International Mechanical Engineering Conferences and Exposition*, Chicago (IL, USA), Nov 2006.

[2] Cartmell M.: *Introduction to Linear, Parametric and Nonlinear Vibrations*. Chapman & Hall, London, 1990.

[3] Tondl A.: "On the Interaction between Self-Excited and Parametric Vibrations". *Monographs & Memoranda*, Vol. 25, National Research Institute for Machine Design, Prague, l978.

[4] Tondl A.: "To the Problem of Quenching Self-Excited Vibrations". *Acta Technica ČSAV*, Vol. 43, 1998.

[5] Tondl A., Ecker H.: "Cancelling of Self-Excited Vibrations by Means of Parametric Excitation". *Proceedings of ASME 1999 Design Engineering Technical Conference*, Las Vegas (NV, USA), Sept 1999.

[6] Dohnal F.: *Damping of Mechanical Vibrations by Parametric Excitation*. Doctoral Thesis, Vienna University of Technology, 2005.

[7] Paradeiser W.: *Experimenteller Nachweis einer Parameter-Antiresonanz*. Diploma Thesis (in German), Vienna University of Technology, 2006.

[8] Silvester P.P., Ferrari R.L.: *Finite Elements for Electrical Engineers*. Cambridge University Press, Cambridge (UK), 1996.

[9] Bastos J.P.A., Sadowski N.: *Electromagnetic Modeling by Finite Element Methods*. Marcel Dekker Ltd, New York (USA), 2003.

[10] Jin J.: *The Finite Element Method in Electromagnetics*. John Wiley & Sons, New York (USA), 2002.

[11] Moon F.C.: *Magneto Solid Mechanics*. John Wiley & Sons, London, 1993.